A Framework to Determine Secure Distances for Either Drones or Robots Based Inventory Management Systems

BUDI RAHMADYA[1,2]**, RAN SUN**[1]**, (Member, IEEE), SHIGEKI TAKEDA**[1]**, (Member, IEEE), KENICHI KAGOSHIMA**[1]**, (Life Fellow, IEEE), AND MASAHIRO UMEHIRA**[1]**, (Member, IEEE)**
[1]Graduate School of Science and Engineering, Ibaraki University, Hitachi 316-8511, Japan
[2]Department of Computer Engineering, Faculty of Information and Technology, Andalas University, Padang 25175, Indonesia

Corresponding author: Shigeki Takeda (shigeki.takeda.tmkyou@vc.ibaraki.ac.jp)

ABSTRACT We propose a framework to determine a secure distance between a drone with an ultrahigh-frequency band radio frequency identification (UHF band RFID) reader and metallic objects affixed with RFID tags. The secure distance avoids order changes in received signal strength indicator (RSSI) values among the identified RFID tags in the field of view of the RFID reader. This distance enables a drone operator to securely operate the drone while identifying the RFID tag on the front of an object based on the measurements of RSSI values. An RFID tag located on the front of an object provides the maximum RSSI value. However, multipath propagation alters the RSSI values. Therefore, a framework is needed to determine a secure distance considering the multipath effects. Although inventory management systems based on drones and RFID systems been proposed to date, this article establishes a framework to determine the secure distance. In the proposed framework, RFID tag and reader radiation patterns and multipath propagation effects were considered. The proposed framework was evaluated theoretically and experimentally. To evaluate and demonstrate the secure distance, we measured the RSSI values of two RFID tags attached to a metallic balcony. The height from the ground and spacing of the two RFID tags were 1.5 m and 1.3 m, respectively. In this environment, the secure distance was 3.8 m. The experimentally obtained distance that avoids order changes in RSSI values corresponded well with that obtained by this framework. The proposed secure distance is crucial when either drones or robots are introduced to inventory management systems.

INDEX TERMS Drone, robot, secure distance, UHF RFID, RSSI, inventory management, metallic object.

I. INTRODUCTION

Currently, mobile devices such as unmanned aerial vehicles (UAVs) or drones are increasingly gaining popularity because they can be easily operated with remote controls. Furthermore, drones and robots have been introduced to many fields of endeavor such as inventory management systems. Drones utilizing ultrahigh-frequency band radio frequency identification (UHF band RFID) systems are effective wireless devices for applications such as identifying and locating objects in a wide area, including indoor and outdoor warehouses. RFID tags do not require internal batteries and are inexpensive. In [1]–[5], practical inventory

The associate editor coordinating the review of this manuscript and approving it for publication was Renato Ferrero .

management systems for warehouses and libraries based on drones and robots have been developed. In [6]–[10], signal and video processing techniques for drones have been presented. In [11]–[13], RFID techniques have been combined with drones, and electromagnetic wave propagation characteristics have been clarified. As discussed, drones have the potential to be effective devices in conjunction with RFID systems, and practical applications have been studied. In [14]–[19], the location and identification systems of various objects based on RFID systems and drones have been presented. In [20]–[23] techniques for safe operation of drones have been discussed, and in [24]–[28], routing techniques for drones have been presented. In [29] and [30], synthetic aperture (SAR) has been applied to identify RFID tag-affixed objects in a warehouse. In addition, in drone-based inventory

IEEE Access

B. Rahmadya *et al.*: Framework to Determine Secure Distances for Either Drones or Robots Based Inventory Management Systems

management systems, compact RFID reader antennas are in demand because the drone needs to carry the RFID reader. Many compact RFID reader antennas have been proposed in [31]–[34], and they are effective in drone-based inventory management systems because compact and lightweight RFID readers are required, as mentioned above. Furthermore, dual-band RFID integrated circuit (IC) and card-type antennas have been developed in [35] and [36]. Because these RFID tags can communicate with both UHF RFID and near-field communication (NFC) readers, the use of these thin and compact RFID tags is effective in inventory management systems. These RFID tags enable warehouse staff to communicate with RFID tags with NFC-equipped standard smart phones.

Thus, a question arises as to the required distance between a drone and objects in a warehouse affixed with RFID tags [5]. A drone should maintain a certain distance from these objects to avoid a collision. However, the drone should be close enough to the front object to detect the electronic product code (EPC) based on the measurements of received signal strength indicator (RSSI) values. In particular, if the distance is short, an RFID tag located in front of the RFID reader backscatters the maximum RSSI value. Conversely, when the distance increases, the relative distances between an RFID reader and RFID tags presented in the field of view of an RFID reader become comparable. This effect causes magnitude order changes among the observed RSSI values because multipath propagation alters the RSSI values. The RFID reader becomes confused because it cannot identify the true EPC of the RFID tag, which is obtained by camera images. The RFID reader may relate an incorrect EPC with the camera image. Therefore, a framework is required to determine the boundary distance that enables secure drone operation and reliable target RFID tag detection, herein deemed the secure distance [37]. This article presents a framework, which was evaluated experimentally, to determine the secure distance. As we mentioned before, [1]–[5] developed practical drones and robot-based systems, and [11]–[13] and [30] studied electromagnetic propagation effects and the use of SAR techniques. Although many inventory management systems based on drones and RFID systems have been proposed to date, this article establishes the framework to determine the secure distance. In the proposed framework, the RFID tag and reader radiation patterns and multipath propagation effects were considered.

II. APPLICATION EXAMPLES

The system model is illustrated in Fig. 1. Figures 1 (a) and (b) show drone- and robot-based inventory management systems, respectively.

RFID-based automated inventory management systems utilizing a drone with an RFID reader are presented in Fig. 1 (a). Metallic objects with RFID tags are assumed here. The warehouse manager controls the drone using a remote controller and observes video images that are transmitted from the drone. The drone is equipped with an RFID reader and
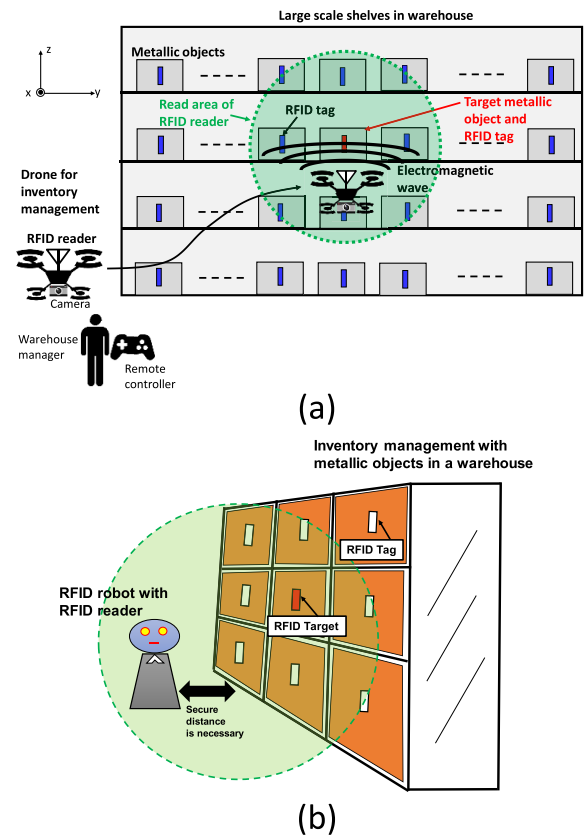

FIGURE 1. System models. (a) Inventory management with a drone in a warehouse. (b) Inventory management with an RFID robot in a warehouse.

a camera. The camera identifies an object in front of it using image processing technology, whereas the RFID reader identifies the EPC numbers of RFID tags in its field of view. Generally, to identify the EPC number of the front RFID tag, an RSSI measurement is convenient. If the distance between the drone and object is short, the RSSI, which is backscattered from the front RFID tag, provides the maximum values. However, short distances are dangerous because they make drones prone to collision with objects. On the other hand, longer distances, albeit safe, will lead to comparable RSSI values from the RFID tags. This makes it difficult to identify the RFID tag based on the RSSI measurement. Therefore, a framework to determine the distance between objects and the drone, herein referred to as a secure distance, is required.

An RFID robot for inventory management is illustrated in Fig. 1 (b). Each box has an RFID tag, and the RFID robot is equipped with an RFID reader. The RFID robot scans the boxes to find the target RFID tag based on maximum RSSI measurements. However, similar to the case of the drone shown in Fig. 1 (a), a secure distance for localizing the front RFID tag based on the RSSI measurement is necessary.

III. DESIGN FRAMEWORK OF SECURE DISTANCES

This section presents a framework for determining a secure distance. The framework consists of the following steps:
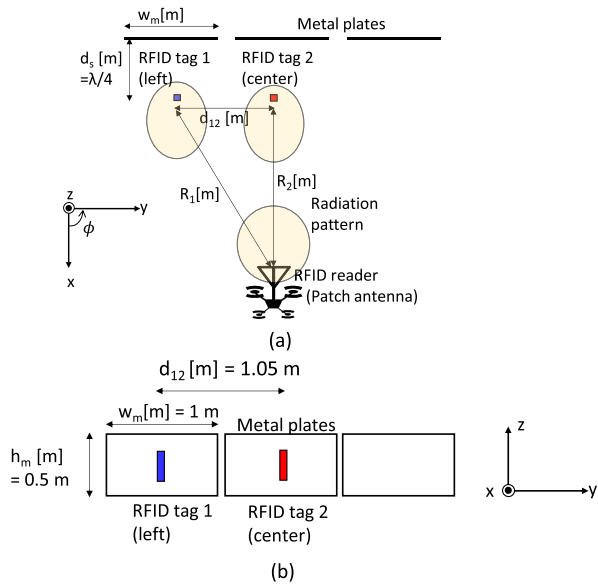
B. Rahmadya *et al.*: Framework to Determine Secure Distances for Either Drones or Robots Based Inventory Management Systems

IEEE *Access*

FIGURE 2. Geometry of the drone-based inventory management system. (a) x-y plane. (b) z-y plane.

preparing an analytical model, computing antenna radiation patterns, calculating backscattered received power values using the radar equation, obtaining fading margin values, and estimating a fading variation using a ray tracing simulation. After explaining each step, the aforementioned procedure is summarized in a flowchart.

Figure 2 shows an analytical model of an RFID and drone-based warehouse management system. Figure 2 (a) shows the analytical model in the x-y plane. To evaluate the difference between backscattered RSSI values, two RFID tags are placed: one is placed in front of the drone, and the other deviates from the center, as RFID tags 1 (left) and 2 (center). The metallic objects are modeled as reflecting metallic plates for simplicity, where the distances between the RFID tags and metal plates, d_s, are a quarter of a wavelength in the free space to form single-beam radiation patterns toward the front. R_1 and R_2 denote the distances between the RFID reader antenna and the RFID tags, respectively, while w_m and d_{12} denote the widths of the metal plates and the spacing between the RFID tags, respectively. A typical patch antenna was assumed in this model because the antenna geometry of the RFID reader used in the later experimental part is unknown.

Figure 2 (b) shows an analytical model in the z-y plane. To obtain the received power values, radiation patterns of the RFID tags with the metallic plates were computed by an electromagnetic field simulator. A SHORT DIPOLE RFID tag with Impinj Monza 4D, provided by Smartrac, was modeled as RFID tag antennas in this simulation. The dimensions of the metallic plates were 0.5 m in height h_m and 1 m in width w_m. The spacing between the RFID tags, d_{12}, was 1.05 m.

The backscattered received power values from RFID tag 1 and tag 2 are obtained by the following radar equation
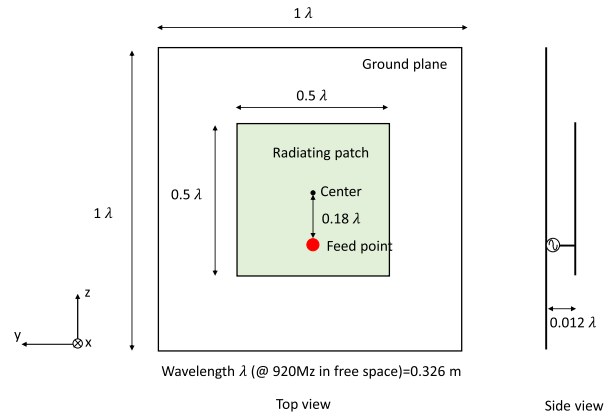

Wavelength λ (@ 920Mz in free space)=0.326 m

FIGURE 3. RFID reader antenna model.

modified for RFID systems [38], [39]:

$$P_r = \frac{P_t G_t^2 \lambda^2 \Delta\sigma}{(4\pi)^3 R^4} \qquad (1)$$

$$\Delta\sigma = \frac{\lambda^2 G_{tag}^2}{4\pi} \qquad (2)$$

where P_t, G_t, λ, and G_{tag} denote an RFID reader's transmit power value and antenna gain, wavelength at 920 MHz, and tag antenna gain, respectively. R denotes the distance between the RFID reader and the tag. Note that a differential radar cross section $\Delta\sigma$ was obtained by assuming a load modulation between matched and short-circuited loads [39].

To obtain the received power values of the RFID reader antenna, radiation patterns of the RFID tags with the metallic plates are computed by an EEM-MOM version 3.0 electromagnetic field simulator [40].

Figure 3 shows the antenna geometry of an RFID reader antenna assumed in this study. This typical patch antenna comprises a one-wavelength square ground plane and a half-wavelength square fed patch element. To achieve impedance matching for 50 Ω, a feed point deviates from the center of the patch element. The obtained voltage standing wave ratio (VSWR) at a frequency of 920 MHz was less than 1.5. The patch element is excited between the ground plane and patch element.

The obtained radiation patterns of RFID tag 1 and tag 2 in the x-y plane are displayed in Fig. 4. These antennas form single beams toward a straight direction ($\phi = 0°$) owing to the presence of the reflectors shown in Fig. 2. Both RFID tags have nearly identical radiation patterns. Figure 5 presents the radiation pattern of the patch antenna shown in Figure 3. To conform to the regulations in Japan, when these antenna gains are substituted into the radar equation, the use of an attenuator is assumed, and the maximum gain is reduced to 3 dBi. The half-power beam widths (HPBWs) in the E-plane and H-plane are 56° and 59°, respectively.

Figure 6 demonstrates received power values obtained using the radar equations shown in (1) and (2), where antenna gains are obtained by the radiation patterns shown
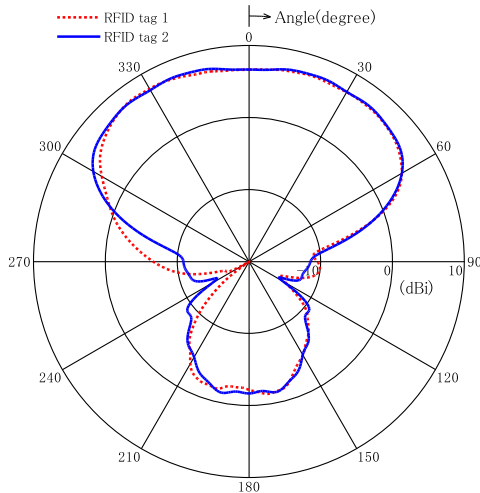
IEEE *Access*

B. Rahmadya *et al.*: Framework to Determine Secure Distances for Either Drones or Robots Based Inventory Management Systems

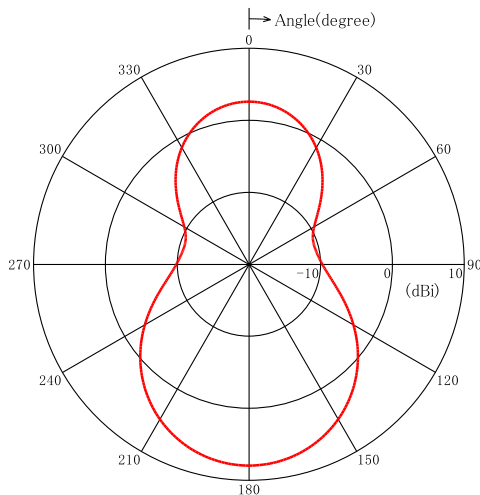**FIGURE 4.** Radiation patterns of RFID tag 1 and RFID tag 2 in the x-y plane.

FIGURE 5. Radiation pattern of the patch antenna shown in Fig. 3.

in Figs. 4 and 5. The backscattered power values from RFID tag 2 vary only when depending on the distance R_2 because the antenna gains of the RFID reader and RFID tag 2 are always constant. Conversely, as the antenna gains of RFID tag 1 and the RFID reader vary depending on the distance R_1, the radiation patterns of RFID tag 1 and RFID reader affect the curve of the backscattered power P_{r1}. Since the P_{r1} curve gradually converges to that of P_{r2}, the RFID reader cannot discriminate the RFID tag in front of it from the adjacent ones based on the maximum RSSI measurements. Therefore, the drone must be closer to the target RFID tag to obtain the maximum RSSI value. In Figure 6, for example, the distance providing 3 dB differences is indicated by the vertical blue dashed line at 2.8 m. This difference should be chosen to make the difference between the RSSI values greater than the variations caused by multipath fading. The fading margin values are indicated by the dotted green line. In the latter section, studies on the fading variations will be given based on
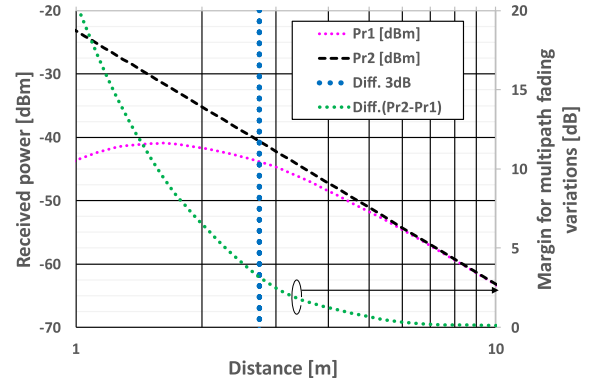

FIGURE 6. Obtained received power values using the radar equations and radiation patterns shown in Figures 4 and 5.

analyses using a ray-tracing simulator. Hence, by conducting ray-tracing simulation, we can determine a secure distance in a given environment.

Secure distances for different spacings from that of $d_{12} = 1.05$ m were evaluated. The widths of the metal plates were changed while keeping the spacing between the metal plates at 5 cm. The widths of the newly evaluated metal plate sizes were 0.25 m, 0.50 m, 0.75 m, 1.25 m, and 1.50 m. Therefore, the spacings, d_{12}, were 0.30 m, 0.55 m, 0.80 m, 1.30 m, and 1.55 m. For d_{12} values of 1.30 m and 1.55 m, radiation patterns were evaluated with similar simulation models as that of $d_{12} = 1.05$ m. On the other hand, several metal plates were added on both sides to reduce edge effects for the cases in which d_{12} values are less than or equal to 0.80 m, as shown in Fig. 7 (a). Figure 7 (a) shows secure distances as a function of d_{12} and Fig. 7 (b) shows radiation patterns for each d_{12} value. Because the radiation patterns for $d_{12} = 1.05$ m have already been shown in Fig. 4, they were omitted in this graph. In addition, the center value in Fig. 7 (b) was changed from that of Fig. 4 to enlarge the differences around the 0° direction. When the spacings d_{12} are greater than or equal to 1.05 m, the secure distances are unchanged and are approximately 2.8 m. This is because the radiation patterns shown by the colors red and blue in Fig. 7 (b) are almost the same as those of $d_{12} = 1.05$ m. In contrast, the radiation patterns are altered depending on the spacing d_{12} and the widths of the metal plates when d_{12} values are less than or equal to 0.80 m. Because the radiation patterns for d_{12} of 0.8 m and 0.3 m become concave around the 0° direction, these characteristics reduce the secure distances. On the other hand, because the radiation pattern becomes convex around the 0° direction, this increases the secure distance.

Figure 8 shows a flow chart of the proposed framework to determine a secure distance.

IV. EXPERIMENTAL VALIDATION OF THE PROPOSED FRAMEWORK

To validate the analytical framework presented in the previous section, two RFID tags were affixed to a metallic balcony, and they were read by an RFID reader. Figure 9 shows the experimental environment and setups. The experiment was
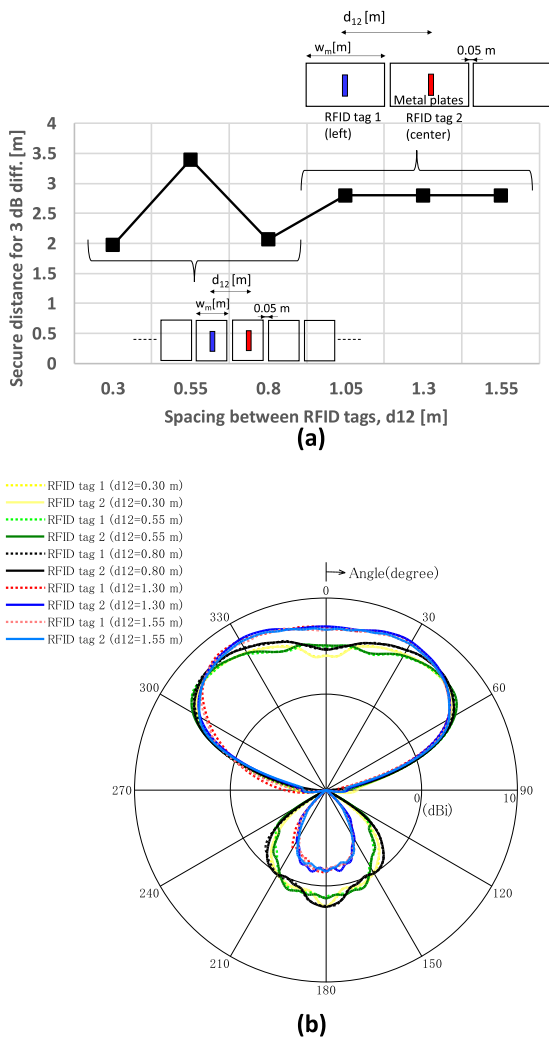
B. Rahmadya *et al.*: Framework to Determine Secure Distances for Either Drones or Robots Based Inventory Management Systems

IEEE *Access*

FIGURE 7. Secure distances as a function of spacings between RFID tags. (a) Secure distance for d_{12}. (b) Radiation patterns for d_{12}.
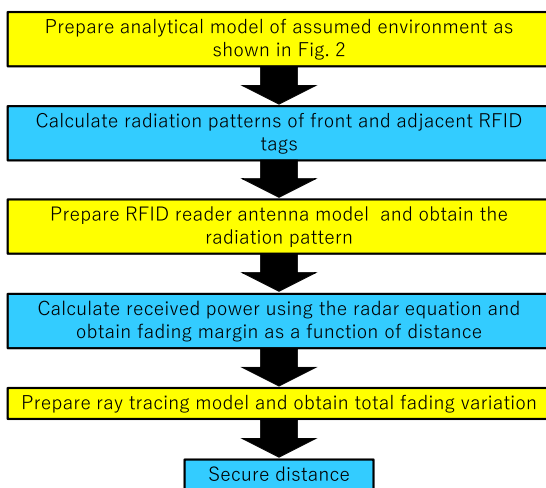

FIGURE 8. Flow chart of the proposed framework used to determine a secure distance.

carried out on a balcony at the international student dormitory for the engineering faculty of Ibaraki University. RFID tag 1 and tag 2 were installed on a balcony made of metal. The
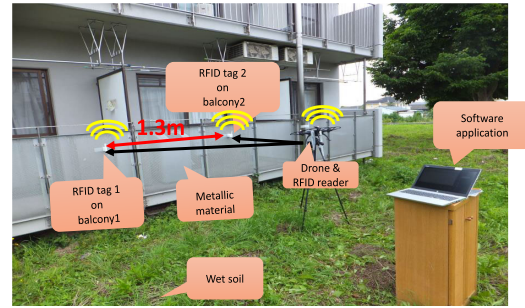

FIGURE 9. Experimental environment. (a) Experimental setup. (b) RFID reader installed on the drone.

TABLE 1. Specifications for an RFID reader, RFID tag, and drone.

Device	Specification
RFID reader	DOTR-910j (250 mW) 920 MHz
RFID tag	SHORT DIPOLE, Impinj Monza 4D, EPC:300000000000000000000000213(left), EPC:300000000000000000000000214(center)
Drone	Holy stone HS 300

distance between these two RFID tags is 1.3 m, and the height of the drone with an RFID reader is 1.5 m. A DOTR-910J was used [41], which has a radiation power of 250 mW and is equipped with a circularly polarized antenna. A software development kit (SDK) was provided with the RFID reader, and the developed SDK was used to record the RSSI values. The RFID reader is connected with a laptop computer via a Bluetooth connection. Table 1 shows the specifications of the RFID reader, RFID tag, and drone. The RFID reader was installed with the drone to consider electromagnetic effects by the drone. The drone and RFID reader were supported by a tripod. The RFID reader was too heavy to be carried by the drone. Therefore, a lightweight RFID reader will be required to keep the drone stable. The assumed drone in our experiment was HS300, and this drone can fly for approximately 8 to 10 minutes without changing a battery according to a manual book. For example, if we assume a 1 m/s velocity for reliable RFID readings, the effective distance of the drone is estimated to be $1 \times (8 \times 60) = 480$m. If the spacing of RFID tags is 1.05 m, which is assumed in Fig 2 (b), the drone can roughly identify $480/1.05 \approx 457$ RFID tags. The diameter of the drone is approximately 60 cm, and a secure distance must be longer than the radius of the drone.
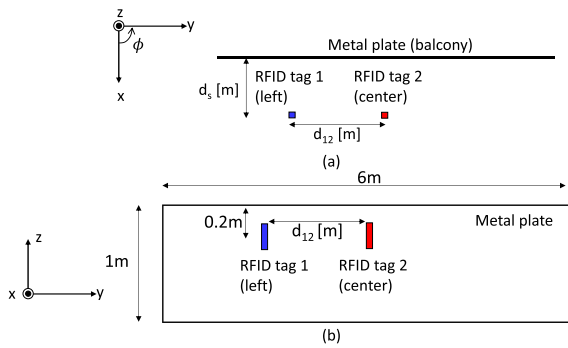
FIGURE 10. Electromagnetic wave simulation environment. (a) x-y plane. (b) z-y plane.
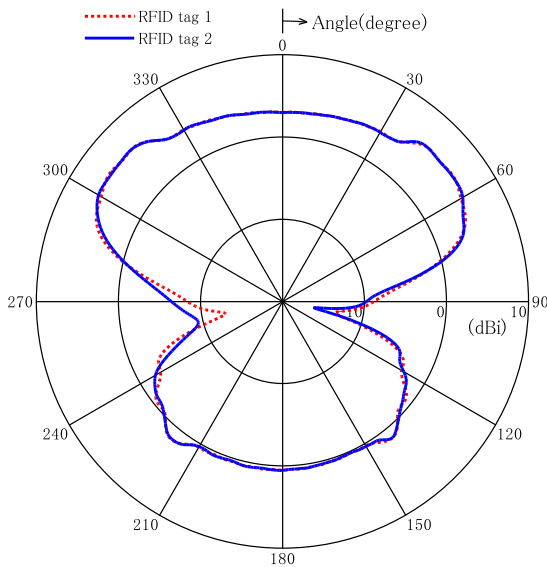

FIGURE 11. Radiation pattern of RFID tag 1 and tag 2 in the x-y plane for the metallic balcony environment.

Figure 10 displays the electromagnetic wave simulation environment of RFID tag 1 and tag 2 in the x-y and z-y planes, respectively. The electromagnetic wave simulation environment of the RFID tags affixed to the metallic balcony to evaluate the backscattered power values from RFID tag 1 and tag 2. d_{12} is 1.3 m. The same patch antenna as shown in Figure 3 is used as an RFID reader antenna. Radiation patterns of the two RFID tags are obtained with this model by electromagnetic analyses using [40]. The metal plate size in the computer simulation is 6 m × 1 m, and d_s was set to be $\frac{\lambda}{4}$ to form a single beam of radiation toward the front direction. Radiation patterns of the two RFID tags are obtained in this model using electromagnetic wave analyses and are shown in Fig. 11. The HPBWs of the E-plane and H-plane are 150° and 100°, respectively.

Figure 12 (a), (b) and (c) show the measured average RSSI values of RSSI1 (RFID tag 1) and RSSI2 (RFID tag 2), box-and-whisker plots of the measured results, and success rates satisfying the condition of (RSSI2 > RSSI1), respectively. The RSSI values were measured four times at
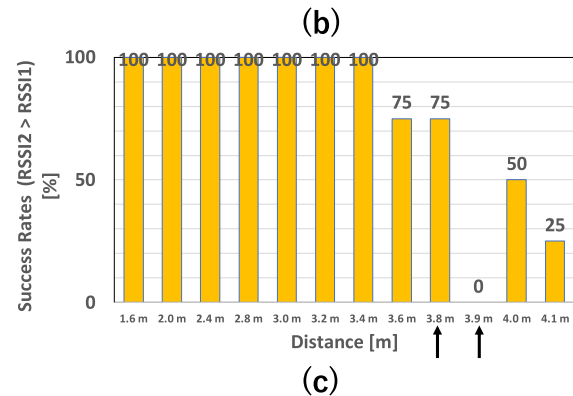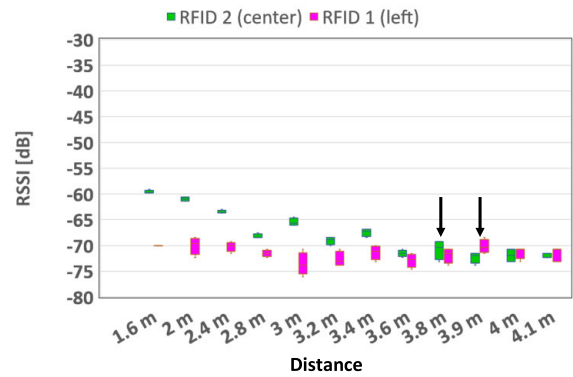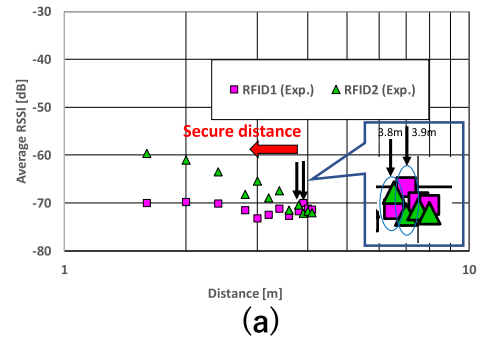

FIGURE 12. Measured results as a function of distance. (a) Average RSSI values of RSSI1 (RFID tag 1) and RSSI2 (RFID tag 2). (b) Box-and-whisker plots of the measured results. (c) Success rates in the case of (RSSI2 > RSSI1).

each distance. In Fig. 12 (a), when the distances are less than 3 m, average RSSI values with larger differences are obtained. On the other hand, RSSI1 and RSSI2 draw closer at 3.8 m. Furthermore, at 3.9 m, their order of magnitude is changed. These phenomena are caused by multipath propagation, and simulation results on this effect are evaluated later. To avoid the changes in order of magnitude in RSSI values and detect the RFID tag in the front based on RSSI measurements, a sufficient margin value is required between the RSSI values. This margin value determines the distance that avoids the changes in order of magnitude in RSSI values while keeping a drone safe. This distance corresponds to the secure distance in this experimental environment. In this environment, a distance of approximately 3.8 m is considered a secure distance. Fig. 12 (b) shows the distributions of the experimental results. At 3.9 m, all the RSSI2 values were
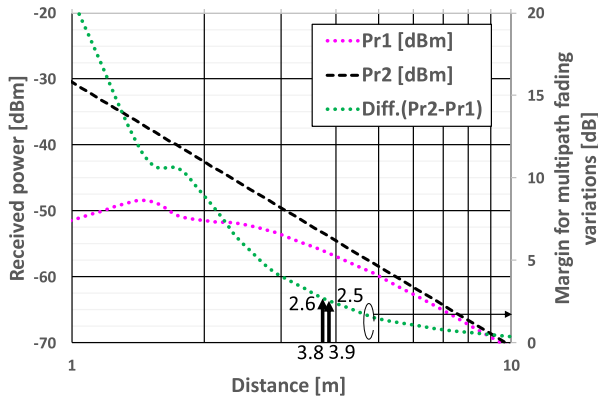
B. Rahmadya *et al.*: Framework to Determine Secure Distances for Either Drones or Robots Based Inventory Management Systems

IEEE *Access*

FIGURE 13. Theoretically obtained received power values of RFID tag 1 and tag 2 in the balcony environment as a function of distance.

less than those of RSSI1. Figure 12 (c) shows the success rates. At 3.9 m, the success rate was significantly decreased, and the success rates decreased when increasing this distance.

Figure 13 displays theoretically obtained received power values of RFID tag 1 and tag 2 in the balcony environment as a function of distance. The analytical framework presented in Fig. 2 was used. In the experimental data shown in Fig. 12 (a), the order change in RSSI values was observed at 3.9 m, and the difference at 3.9 m in Fig.13 was approximately 2.5 dB. This distance depends on the wireless propagation environment. Therefore, wireless propagation channel characteristics should be experimentally or analytically evaluated in advance to determine the margins. At 3.8 m, the difference is 2.6 dB. Wireless propagation channel characteristics are obtained using a ray-tracing simulator [42]- [44] to finally estimate a secure distance.

An RFID reader referred to as DOTR-910J was used in our experiment. This RFID reader provides an RSSI in dB. The manual does not provide the relationship between the RSSI and received power in dBm. Therefore, the experimentally obtained RSSI values of RFID tag 2 in Fig. 12 (a) are compared with the theoretically obtained received power values in Fig. 13. These results confirmed that the RSSI values are proportional to the received power values because the differences between them are approximately constant. The average of the differences was 18 dB. Namely, because adding 18 dB to RSSI values provides received power values, the reference value is 0 dBm $= -18$ dB.

Figure 14 displays a model of the ray-tracing simulation environment between Tx and Rx [42]. To determine the variations caused by multipath fading phenomena in the environment shown in Figure 9, the simulation model consists of transmit and receive antennas (Tx and Rx antennas) and a ground. With this model, interferences between the line of sight (LOS) and ground reflected waves are evaluated [42]–[44]. This is because LOS and ground reflected paths are considered major factors in the experimental environment shown in Fig. 9. The ground is wet soil. The relative permittivity and conductivity values are 20 and
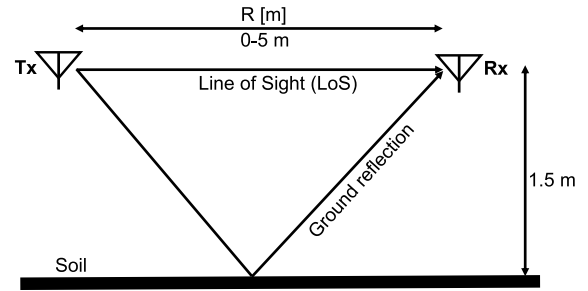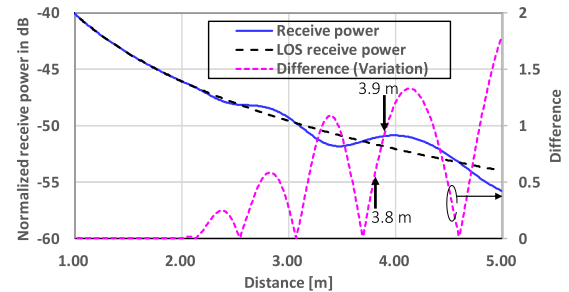

FIGURE 14. Model of ray-tracing simulation between Tx and Rx.

Distance	From this figure				From Fig. 13	
	One way fluctuation [dB]	Round trip fluctuation [dB]	Total fading variation [dB]		Fading margin [dB]	Order change on RSSI
3.9 m	0.93	1.86	3.72	>	2.5	Occur
3.8 m	0.53	1.06	2.12	<	2.6	Not occur

FIGURE 15. Normalized received power obtained by the ray-tracing simulation as a function of distance.

0.01, respectively [45]. The beam width of the antennas is determined by the radiation pattern in Figs. 11 and 5.

Figure 15 shows the normalized received power obtained by the ray-tracing simulation [45] based on the distance. The received power and the LOS received power curves are almost similar for distances from 0 to 2 m. Subsequently, the received power values begin to fluctuate at distances greater than 2 m. This fluctuation is caused by the interferences between the LOS and ground reflected waves. The right axis indicates absolute values of the differences. Since round-trip propagation must be considered in RFID systems, fluctuations become double [44] of those for the one-way propagation. At 3.9 m, the difference is approximately 0.93 dB, which causes approximately 1.86 dB fluctuations for round-trip propagation. Furthermore, since RFID tag 1 and tag 2 both fluctuate, the total fading variation becomes 3.72 dB. This value is greater than 2.5 dB in Fig. 13 at a distance of 3.9 m. This ray-tracing simulation validates Figs. 12 and 13. At 3.8 m, the variation is 0.53 dB in this figure, which becomes double when considering round-trip propagation, 1.06 dB. Furthermore, the total fading variation at 3.8 m is estimated to be 2.12 dB by considering variations of both RFID tags. In Fig. 13, the fading margin is approximately 2.6 dB, which is greater than the total fading variation. Therefore, changes in order of magnitude in RSSI values did not occur at 3.8 m. Hence, 3.8 m is considered a secure distance. The table in Fig. 15 summarizes these studies.

IEEE *Access*

B. Rahmadya *et al.*: Framework to Determine Secure Distances for Either Drones or Robots Based Inventory Management Systems

V. CONCLUSION

In this article, a framework is proposed to obtain a secure distance between a drone and an RFID-tag-affixed metallic object in automated warehouse inventory management systems. The secure distance is defined to avoid order changes in RSSI values among the identified RFID tags presented in the field of view of the RFID reader. This distance provides a stable maximum RSSI value from the target in front of the drone while keeping the drone safe. Therefore, the secure distance enables a drone operator to securely operate the drone while identifying an RFID tag on the front of an object based on the measurements of RSSI values. The framework consists of radiation pattern analyses of the RFID tags and RFID reader, backscattered received power analyses based on the radar equation, and propagation channel analyses. In this study, the propagation channel characteristics are obtained by a ray-tracing simulation, and fluctuations of received power caused by multipath fading phenomena are also obtained. A two-ray interference model was used in the ray-tracing analyses. The proposed framework was evaluated experimentally. The distance that avoids order changes in RSSI values backscattered by the RFID tags in the field of view of the RFID reader corresponded well with that obtained by the framework. The proposed secure distance will be crucial when drones and robots are introduced to warehouse management.

REFERENCES

[1] *Automated Robot*. Accessed: Aug. 31. [Online]. Available: https://phys.org/news/2016-06-automated-robot-scans-library-shelves.html

[2] *I Robot Can Help You Librarian*. Accessed: Aug. 31. [Online]. Available: http://library.ifla.org/2699/1/s08-2019-chakarova-en.pdf

[3] *Drones Relay RFID Signals for Inventory Control*. Accessed: Aug. 31. [Online]. Available: http://news.mit.edu/2017/drones-relay-rfid-signals-inventory-control-0825

[4] Laxcen. *RFID Smart Inventory Robot*. Accessed: Aug. 31. [Online]. Available: http://www.laxcen.com/en/product.php?tid=397

[5] *Drone Automation For Warehouse 4.0*. Accessed: Aug. 31. [Online]. Available: https://cdn.flytbase.com/wp-content/uploads/2019/04/Drone-Automation-in-Warehouse-4.0.pdf

[6] R. Hamatapa and C. Vongchumyen, "Image processing for drones detection," in *Proc. 5th Int. Conf. Eng., Appl. Sci. Technol. (ICEAST)*, Jul. 2019, pp. 1–4.

[7] W. Budiharto, A. A. S. Gunawan, J. S. Suroso, A. Chowanda, A. Patrik, and G. Utama, "Fast object detection for quadcopter drone using deep learning," in *Proc. 3rd Int. Conf. Comput. Commun. Syst. (ICCCS)*, Apr. 2018, pp. 192–195.

[8] M. Nalamati, A. Kapoor, M. Saqib, N. Sharma, and M. Blumenstein, "Drone detection in long-range surveillance videos," in *Proc. 16th IEEE Int. Conf. Adv. Video Signal Based Surveill. (AVSS)*, Sep. 2019, pp. 1–6.

[9] B. Taha and A. Shoufan, "Machine learning-based drone detection and classification: State-of-the-art in research," *IEEE Access*, vol. 7, pp. 138669–138682, 2019.

[10] Y.-P. Huang, L. Sithole, and T.-T. Lee, "Structure from motion technique for scene detection using autonomous drone navigation," *IEEE Trans. Syst., Man, Cybern. Syst.*, vol. 49, no. 12, pp. 2559–2570, Dec. 2019.

[11] G. Casati, M. Longhi, D. Latini, F. Carbone, S. Amendola, F. D. Frate, G. Schiavon, and G. Marrocco, "The interrogation footprint of RFID-UAV: Electromagnetic modeling and experimentations," *IEEE J. Radio Freq. Identificat.*, vol. 1, no. 2, pp. 155–162, Jun. 2017.

[12] M. Longhi and G. Marrocco, "Flying sensors: Merging nano-UAV with radiofrequency identification," in *Proc. IEEE Int. Conf. RFID Technol. Appl. (RFID-TA)*, Sep. 2017, pp. 164–168.

[13] M. Longhi, G. Casati, D. Latini, F. Carbone, F. D. Frate, and G. Marrocco, "RFIDrone: Preliminary experiments and electromagnetic models," in *Proc. URSI Int. Symp. Electromagn. Theory (EMTS)*, Aug. 2016, pp. 450–453.

[14] L. Shen, Q. Zhang, J. Pang, H. Xu, and P. Li, "PRDL: Relative localization method of RFID tags via phase and RSSI based on deep learning," *IEEE Access*, vol. 7, pp. 20249–20261, 2019.

[15] S. Siachalou, S. Megalou, A. Tzitzis, E. Tsardoulias, A. Bletsas, J. Sahalos, T. Yioultsis, and A. G. Dimitriou, "Robotic inventorying and localization of RFID tags, exploiting phase-fingerprinting," in *Proc. IEEE Int. Conf. RFID Technol. Appl. (RFID-TA)*, Sep. 2019, pp. 362–367.

[16] S. Sanyal, S. Bhushan, and K. Sivayazi, "Detection and location estimation of object in unmanned aerial vehicle using single camera and GPS," in *Proc. 1st Int. Conf. Power, Control Comput. Technol. (ICPC2T)*, Jan. 2020, pp. 73–78.

[17] S. G. Sammeta and S. R. Madara, "Recent trends in RFID technologies and its impact on universities," in *Proc. Adv. Sci. Eng. Technol. Int. Conf. (ASET)*, Feb. 2018, pp. 1–6.

[18] C.-H. Yang and H.-M. Tsai, "Vehicle counting and speed estimation with RFID backscatter signal," in *Proc. IEEE Veh. Netw. Conf. (VNC)*, Dec. 2019, pp. 1–8.

[19] P. M. B. Mansingh, T. J. Titus, and V. S. S. Devi, "A secured biometric voting system using RFID linked with the Aadhar database," in *Proc. 6th Int. Conf. Adv. Comput. Commun. Syst. (ICACCS)*, Mar. 2020, pp. 1116–1119.

[20] H. Huang, A. V. Savkin, and C. Huang, "Reliable path planning for drone delivery using a stochastic time-dependent public transportation network," *IEEE Trans. Intell. Transp. Syst.*, early access, Apr. 7, 2020, doi: 10.1109/TITS.2020.2983491.

[21] M. Nalamati, A. Kapoor, M. Saqib, N. Sharma, and M. Blumenstein, "Drone detection in long-range surveillance videos," in *Proc. 16th IEEE Int. Conf. Adv. Video Signal Based Surveill. (AVSS)*, Sep. 2019, pp. 1–6.

[22] E. Vinogradov, F. Minucci, and S. Pollin, "Wireless communication for safe UAVs: From long-range deconfliction to short-range collision avoidance," *IEEE Veh. Technol. Mag.*, vol. 15, no. 2, pp. 88–95, Jun. 2020.

[23] P. Sanjana and M. Prathilothamai, "Drone design for first aid kit delivery in emergency situation," in *Proc. 6th Int. Conf. Adv. Comput. Commun. Syst. (ICACCS)*, Mar. 2020, pp. 215–220.

[24] S. Kim and I. Moon, "Traveling salesman problem with a drone station," *IEEE Trans. Syst., Man, Cybern. Syst.*, vol. 49, no. 1, pp. 42–52, Jan. 2019.

[25] R. A. Nazib and S. Moh, "Routing protocols for unmanned aerial vehicle-aided vehicular ad hoc networks: A survey," *IEEE Access*, vol. 8, pp. 77535–77560, 2020.

[26] H. Seliem, R. Shahidi, M. H. Ahmed, and M. S. Shehata, "Drone-based highway-VANET and DAS service," *IEEE Access*, vol. 6, pp. 20125–20137, 2018.

[27] M. Marinelli, L. Caggiani, M. Ottomanelli, and M. Dell'Orco, "En route truck–drone parcel delivery for optimal vehicle routing strategies," *IET Intell. Transp. Syst.*, vol. 12, no. 4, pp. 253–261, May 2018.

[28] D. Wang, P. Hu, J. Du, P. Zhou, T. Deng, and M. Hu, "Routing and scheduling for hybrid truck-drone collaborative parcel delivery with independent and truck-carried drones," *IEEE Internet Things J.*, vol. 6, no. 6, pp. 10483–10495, Dec. 2019.

[29] A. Buffi, A. Motroni, P. Nepa, B. Tellini, and R. Cioni, "A SAR-based measurement method for passive-tag positioning with a flying UHF-RFID reader," *IEEE Trans. Instrum. Meas.*, vol. 68, no. 3, pp. 845–853, Mar. 2019.

[30] F. Bernardini, A. Buffi, A. Motroni, P. Nepa, B. Tellini, P. Tripicchio, and M. Unetti, "Particle swarm optimization in SAR-based method enabling real-time 3D positioning of UHF-RFID tags," *IEEE J. Radio Freq. Identificat.*, early access, Jun. 30, 2020, doi: 10.1109/JRFID.2020.3005351.

[31] Z. Wang, Y. Dong, and T. Itoh, "Ultraminiature circularly polarized RFID antenna inspired by crossed split-ring resonator," *IEEE Trans. Antennas Propag.*, vol. 68, no. 6, pp. 4196–4207, Jun. 2020.

[32] F.-P. Lai, J.-F. Yang, and Y.-S. Chen, "Compact dual-band circularly polarized antenna using double cross dipoles for RFID handheld readers," *IEEE Antennas Wireless Propag. Lett.*, vol. 19, no. 8, pp. 1429–1433, Aug. 2020.

[33] J. Yuan, S. Wu, Z. Chen, and Z. Xu, "A compact low-profile ring antenna with dual circular polarization and unidirectional radiation for use in RFID readers," *IEEE Access*, vol. 7, pp. 128948–128955, 2019.

[34] L. Sun, Y. Li, Z. Zhang, and Z. Feng, "Low-profile compact circularly polarized slot-etched PIFA using even and odd modes," *IEEE Trans. Antennas Propag.*, vol. 67, no. 6, pp. 4189–4194, Jun. 2019.

B. Rahmadya *et al.*: Framework to Determine Secure Distances for Either Drones or Robots Based Inventory Management Systems

IEEE *Access*

[35] *RAINFC Authenticity Transponder IC*. Accessed: Aug. 31. [Online]. Available: https://www.emmicroelectronic.com/sites/default/files/products/datasheets/4425_DS_02.pdf

[36] M. Alibakhshi-Kenari, R. Ali Sadeghzadeh, M. Naser-Moghadasi, E. Limiti, and B. S. Virdee, "Dual-band RFID tag antenna based on the Hilbert-curve fractal for HF and UHF applications," *IET Circuits, Devices Syst.*, vol. 10, no. 2, pp. 140–146, Mar. 2016.

[37] B. Rahmadya, S. Takeda, K. Kagoshima, and M. Umehira, "Secure distances between a drone and an RFID-tag-afixed metallic object for automated inventory management systems in warehouses," in *Proc. Joint Indo-Jpn. Smart City Symp.*, Oct. 2019. [Online]. Available: http://www.ee.iitm.ac.in/smartcity-2019/program-schedule.pdf

[38] P. V. Nikitin and K. V. S. Rao, "Theory and measurement of backscattering from RFID tags," *IEEE Antennas Propag. Mag.*, vol. 48, no. 6, pp. 212–218, Dec. 2006.

[39] P. V. Nikitin, K. V. S. Rao, and R. D. Martinez, "Differential RCS of RFID tag," *Electron. Lett.*, vol. 43, no. 8, pp. 431–432, Apr. 2007.

[40] *EEM-MOM Version 3.0*, EEM Co. Ltd., Fujimino, Japan. [Online]. Available: http://www.e-em.co.jp/index.html

[41] TSS. *DOTR-910J*. Accessed: Aug. 31. [Online]. Available: https://www.tss21.co.jp/lp/1401900wh/DOTR-900J_wh_catalog.pdf

[42] P. V. Nikitin and K. V. S. Rao, "Antennas and propagation in UHF RFID systems," in *Proc. IEEE Int. Conf. RFID*, Apr. 2008, pp. 277–288.

[43] P. V. Nikitin and K. V. S. Rao, "Performance limitations of passive UHF RFID systems," in *Proc. IEEE Antennas Propag. Soc. Int. Symp.*, Jul. 2006, pp. 1011–1014.

[44] P. V. Nikitin, K. V. S. Rao, and S. Lam, "UHF RFID tag characterization: Overview and state-of-the-art," in *Proc. Antenna Meas. Techn. Assoc. Symp. (AMTA)*, 2012, pp. 1–6.

[45] *EEM-RTM Version 1.4*, EEM Co. Ltd., Fujimino, Japan. [Online]. Available: http://www.e-em.co.jp/index.html

KENICHI KAGOSHIMA (Life Fellow, IEEE) received the B.E., M.E., and Ph.D. degrees in electronics engineering from the Tokyo Institute of Technology, Tokyo, Japan, in 1969, 1971, and 1974, respectively. He joined the Nippon Telegraph and Telephone (NTT) Laboratory, where he engaged in research and development of many kinds of radio communication antennas, especially earth station antennas, satellite borne large multi-beam antennas, and mobile communication antennas. He has served as the Research Group Leader of the Antenna Group, NTT Wireless Systems Laboratories. From 1997 to 2015, he was with the Department of Media and Telecommunications, Ibaraki University, Ibaraki, Japan. He is currently a Professor Emeritus with Ibaraki University. His research interest includes numerical techniques for analyzing complex small antennas and MIMO antennas. He is a Fellow of IEICE, Japan. He received the Yonezawa Prize for Young Engineers in 1973, the Best Paper Award from IEICE in 1998, and the Best Tutorial Paper Award from the Communication Society of IEICE. From 1999 to 2000, he was the Chair of the Technical Committee on Antennas and Propagation of the IEICE. He was also a Secretary and a Treasurer, the Vice Chairman, and the Chairman of the IEEE APS Tokyo-Chapter in 1992, 1993, and 1994, respectively. He was the Chairman of the 2002 International Symposium on Antennas and Propagation (ISAP). He has served as the Session Organizer and the Chairperson of the IEEE Antennas and Propagation Symposium several times. He was an Associate Editor of the *Institute of Electronics, Information and Communication Engineers (IEICE) Transactions on Communications* from 1990 to 1992 and an Editor from 1993 to 1994.

BUDI RAHMADYA received the M.E. degree in computer science from the Nara Institute of Science and Technology (NAIST), Japan, in 2013. He is currently pursuing the Ph.D. degree with the Graduate School of Science and Engineering, Ibaraki University, Ibaraki, Japan. He is currently a Lecturer with the Department of Computer Engineering, Faculty of Information and Technology, Andalas University, Indonesia. His research interests include wireless communications, LPWAN, sensor networks, and remote sensing. He is a member of IEICE, Japan.

RAN SUN (Member, IEEE) received the B.E., M.E., and Ph.D. degrees in computer and information science from Ibaraki University, in 2016, 2017, and 2020, respectively. Since 2020, he has been an Assistant Professor with Ibaraki University. His research interests include optical wireless communication, wireless communication, and error correcting codes. He is a member of IEICE.

SHIGEKI TAKEDA (Member, IEEE) received the B.E., M.E., and Ph.D. degrees in electrical and electronic engineering from Tottori University, Tottori, Japan, in 1996, 1998, and 2000, respectively. Since 2000, he has been with the Department of Media and Telecommunications Engineering, College of Engineering, Ibaraki University, Ibaraki, Japan, where he is currently a Professor. His research interests include RFID tags and antenna systems.

MASAHIRO UMEHIRA (Member, IEEE) received the B.E., M.E., and Ph.D. degrees from Kyoto University, Japan, in 1978, 1980, and 2000, respectively. He joined Nippon Telegraph and Telephone (NTT) Corporation, in 1980, where he was engaged in the research and development of modem and TDMA equipment for satellite communications, TDMA satellite communication systems, broadband wireless access systems for mobile multimedia services, and ubiquitous wireless systems. From 1987 to 1988, he was with the Communications Research Center, Department of Communications, Canada, as a Visiting Scientist. Since 2006, he has been a Professor with Ibaraki University, Hitachi, where he has been the Deputy Dean of the College of Engineering, since 2012. His research interests include broadband wireless access technologies, wireless networking, and cognitive radio technologies for future fixed/nomadic/mobile wireless systems, future satellite communication systems, and ubiquitous services using wireless technologies. He is a Fellow of IEICE, Japan. He is also serving as the President of the IEICE Communications Society, Japan, in 2015. He received the Young Engineer Award and the Achievement Award from IEICE in 1987 and 1999, respectively. He also received the Education, Culture, Sports, Science, and Technology Minister Award in 2001.

• • •